Finally, we have included calculated spectra for a number of other isotopically labeled cyclobutadienes in Tables VI–IX. While Chapman[6] has obtained spectra of two of these, their isotopic purity is such that a comparison with our calculated spectra is not possible.

Acknowledgment. We should like to express our appreciation to the University Research Council, Vanderbilt University which provided travel funds and to the National Academy of Sciences for its endorsement of Dr. Carsky's visit. We are especially grateful to Kaara Ettesvold at the Academy for her efforts in our behalf. We also thank Dr. Péter Pulay for making his program TEXAS available to us.

Registry No. Cyclobutadiene, 1120-53-2; [1,2,3,4-$^2H_4$]cyclobutadiene, 56516-62-2; [1,2-$^2H_2$]cyclobutadiene, 40522-77-8; [1,2-$^{13}C_2$]cyclobutadiene, 84132-26-3; [1,3-$^2H_2$]cyclobutadiene, 84132-27-4; [1,3-$^{13}C_2$]cyclobutadiene, 84132-28-5.

Singlet Energy Transfer from the Charge-Transfer Excited State of Tris(2,2′-bipyridine)ruthenium(II) to Laser Dyes

Krishnagopal Mandal, T. D. L. Pearson, W. P. Krug, and J. N. Demas*

Contribution from the Department of Chemistry, University of Virginia, Charlottesville, Virginia 22901. *Received April 19, 1982*

Abstract: Efficient singlet energy transfer from the charge-transfer (CT) excited state of $[Ru(bpy)_3]^{2+}$ (bpy = 2,2′-bipyridine) to several laser dyes has been demonstrated. The limiting efficiencies of dye singlet state formation are 1.00 which shows the efficiency of formation of the sensitizing state of $[Ru(bpy)_3]^{2+}$ is unity. For most of the dyes in methanol, energy transfer is shown to be predominantly by diffusion-assisted Förster transfer. For Rhodamine 101, however, energy transfer is predominantly by a contact exchange transfer. This result shows that the CT state of the sensitizer has a great deal of singlet character and should be referred to as a spin–orbit state.

Introduction

The photochemical and luminescence properties of $[Ru(bpy)_3]^{2+}$ (bpy = 2,2′-bipyridine) and related complexes with α-diimine ligands are currently under intense investigation.[1-15] These systems are of fundamental interest[1,6,7,9] and are potentially useful for solar energy conversion,[2,4,5,8] for new laser dye systems,[15] and for light intensity measuring systems.[11,12] They exhibit a wealth of excited-state electron-transfer[1-5] and acid–base reactions.[13]

We have previously shown that very efficient singlet energy transfer (~100%) takes place from the emitting charge-transfer (CT) excited state of $[Ru(bpy)_3]^{2+}$ to the lasing singlet state of the dye Rhodamine 101 (Rh101).[14] We have also demonstrated very efficient singlet energy transfer from $[Ru(bpy)_3]^{2+}$ to a variety of laser dyes at very low donor–acceptor concentrations ($\sim 10^{-5}$ M) in solutions in which aggregation is assisted by a suitable surfactant.[15] In this study we provide experimental details of our previous work, new studies on other laser dyes in surfactant-free solutions, and interpretations of the results.

Experimental Section

$[Ru(bpy)_3]Cl_2$ (G. Frederick Smith Chemical Co.) was purified by three recrystallizations from water. The complex was spectroscopically pure as judged from its absorption and emission properties. Laser grade Rhodamine B chloride (RhB), Cresyl Violet acetate (CV), Oxazine 1 nitrate (OX1), and Rhodamine 101 perchlorate (Rh101) from Exciton Chemical Co. were used as received. Nile Blue A chloride (NBA) from Eastman Kodak Chemical Co. was purified by recrystallization from chloroform and was chromatographically pure. Spectroquality solvents were used.

All energy-transfer experiments were carried out using equimolar concentrations of $[Ru(bpy)_3]^{2+}$ and the dyes at room temperature (22 °C). Corrected optically dense excitation spectra were obtained on a microcomputerized luminescence quantum counter comparator.[16] This system is an automated version of our earlier manual instrument.[17] We briefly describe the instrument and its operation; full details are given elsewhere.[16]

The basic quantum counter comparator is shown in Figure 1A. Two 1-cm thick quantum counter cells were mounted side by side in front of the monitoring IR-sensitive photomultiplier tube (PMT) which viewed the sample luminescences from the rear face. Cutoff filters between the sample and the PMT blocked any transmitted excitation light and restricted the spectral region viewed by the PMT to the region of the $[Ru(bpy)_3]^{2+}$ and dye emission. With filters it was not possible to discriminate against the emission contribution from $[Ru(bpy)_3]^{2+}$. The excitation source was directed onto either the unknown sample or the reference quantum counter by an optical beam switcher. Automatic wavelength scans, signal averaging, ratio corrections, and compensation for the nonidealities of the reference quantum counter were all performed under computer control. The reference quantum counter was the previously calibrated optically dense RhB quantum counter (5 g/L in methanol).[17]

In operation the beam switcher alternately illustrated the reference and the sample. Automatic dark current compensation was obtained by deflecting the excitation beam onto a beam stop every cycle and reading the PMT dark current which was subtracted from both the sample and reference signals. The ratio of the sample to reference signals was then calculated. The process was repeated at 10-nm intervals over the 360–590-nm region. This ratio nearly equals the sample's relative photon yield at each wavelength except for the deviations in spectral flatness of the RhB reference counter. The data were then corrected for the small (±4%) variation of the quantum counter to yield the relative photon yield vs. wavelength.

Corrected emission spectra and photon yields were obtained on an SLM 8000 corrected spectrofluorimeter. Correction factors were obtained using a standard lamp.

The luminescence photon yields of $[Ru(bpy)_3]^{2+}$ were determined using the standard optically dilute Parker and Rees method.[18] The

(1) Balzani, V.; Moggi, L.; Manfrin, M. F.; Bolletta, F. *Coord. Chem. Rev.* **1975**, *15*, 321.
(2) Tunuli, M. S.; Fendler, J. H. *J. Am. Chem. Soc.* **1981**, *103*, 2507.
(3) Krishnan, C. V.; Sutin, N. J. *J. Am. Chem. Soc.* **1981**, *103*, 2141.
(4) Lin, C.-T.; Sutin, N. J. *J. Phys. Chem.* **1976**, *80*, 97.
(5) DeGraff, B. A.; Demas, J. N. *J. Am. Chem. Soc.* **1980**, *102*, 6169.
(6) Hipps, K. W.; Crosby, G. A. *J. Am. Chem. Soc.* **1975**, *97*, 7042.
(7) Elfring, W. H.; Crosby, G. A. *J. Am. Chem. Soc.* **1981**, *103*, 2683.
(8) Kelder, S.; Rabani, J. *J. Phys. Chem.* **1981**, *85*, 1637.
(9) Baxendale, J. H.; Rodgers, M. A. *J. Chem. Phys. Lett.* **1980**, *72*, 424.
(10) Krug, W. P.; Demas, J. N. *J. Am. Chem. Soc.* **1979**, *101*, 4394.
(11) Demas, J. N.; McBride, R. P.; Harris, E. W. *J. Phys. Chem.* **1976**, *80*, 2248.
(12) Mandal, K.; Pearson, T. D. L.; Demas, J. N. *Inorg. Chem.* **1981**, *20*, 786.
(13) Peterson, S. H.; Demas, J. N. *J. Am. Chem. Soc.* **1979**, *101*, 6571.
(14) Mandal, K.; Pearson, T. D. L.; Demas, J. N. *J. Chem. Phys.* **1980**, *73*, 2507.
(15) Mandal, K.; Demas, J. N. *Chem. Phys. Lett.* **1981**, *84*, 410.
(16) Pearson, T. D. L.; Cetron, E.; Demas, J. N., in preparation.
(17) Taylor, D. G.; Demas, J. N. *Anal. Chem.* **1979**, *51*, 712, 717.
(18) (a) Demas, J. N.; Crosby, G. A. *J. Phys. Chem.* **1971**, *75*, 991. (b) Demas, J. N. *Anal. Chem.* **1973**, *45*, 992.

0002-7863/83/1505-0701$01.50/0

Table I. Excited-State and Electrochemical Characteristics of Dyes and $[Ru(bpy)_3]^{2+}$ [a]

dye	E_0	$\mathcal{E}^0(S^+/S)$	$\mathcal{E}^0(S/S^-)$	$\Delta\mathcal{E}_{7a}$	$\Delta\mathcal{E}_{7b}$	$\Delta\mathcal{E}_{8a}$	$\Delta\mathcal{E}_{8b}$
Rhodamine 101	2.13	0.88	−1.18	−0.33	−0.10	2.45	2.22
		0.87[b]	−1.15[b]	−0.30	−0.09	2.42	2.21
Cresyl Violet	2.02	1.27	−0.55	0.30	−0.49	1.82	2.61
Nile Blue A	1.90	1.13	−0.40	0.45	−0.35	1.67	2.49
Oxazine 1	1.89	1.19	−0.42	0.43	−0.41	1.69	2.49
$[Ru(bpy)_3]^{2+}$	2.12	1.27	−1.34				

[a] All energies and potentials are given in volts. Electrochemical potentials are referenced to the SCE. All electrochemical measurements were taken in 0.5 M tetrabutylammonium perchlorate. Unless otherwise specified, the solvent was acetonitrile. [b] In methanol.

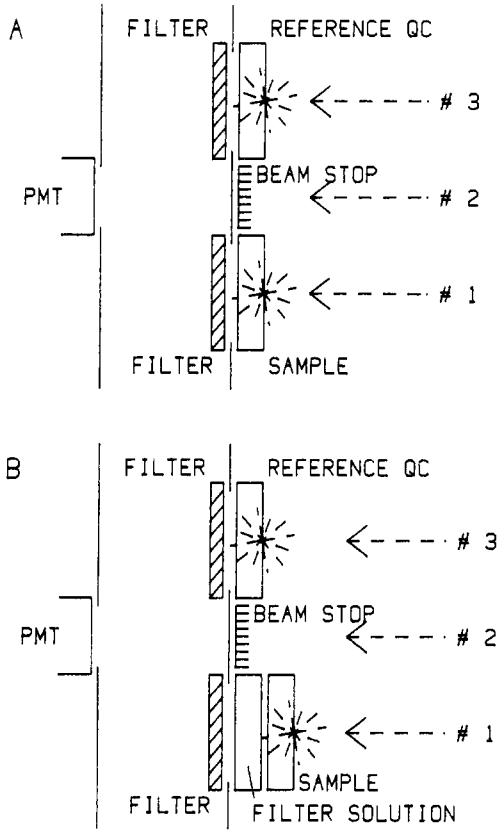

Figure 1. Schematic diagram of the quantum counter (QC) comparator used to measure relative photon yields (A) and effective transmission of the dye solutions (B). A common photomultiplier tube (PMT) views the luminescence from either the sample or the reference QC. The three optical excitation paths are selected by a beam switcher (not shown). In positions 1 and 3, the sample and reference quantum counters are selected, respectively. In position 2, the beam strikes a beam stop for the dark current measurements. The filters block transmitted excited light and can be coupled with neutral density filters to yield comparable PMT signals for the two excitation paths.

standard n^2 refractive index correction was used, and optical densities were kept below 0.05/cm. The photon yield standard was $[Ru(bpy)_3]^{2+}$ in aerated water. Excitation was always at 450 nm which corresponds to the nearly solvent-independent absorption maximum of the complex. This procedure avoided corrections for the spectral variations of the excitation source. The broad spectral characteristics of $[Ru(bpy)_3]^{2+}$ virtually eliminated bandpass errors.[18b] The emission spectrum of the complex is also nearly independent of solvent which minimized any potential errors arising from the instrumental correction factors. The photon yield of the aerated aqueous $[Ru(bpy)_3]^{2+}$ was assumed to be 0.0278. This yield was derived from the 0.042 value reported by Van Houten and Watts for deoxygenated solutions.[19] The degree of oxygen quenching in an air-saturated solution vs. a deoxygenated one was measured and the Van Houten–Watts yield was reduced by the same amount.

Unquenched lifetimes (τ_0's) of $[Ru(bpy)_3]^{2+}$ were measured using a pulsed N_2 laser-microcomputerized nanosecond decay time instrument.[20]

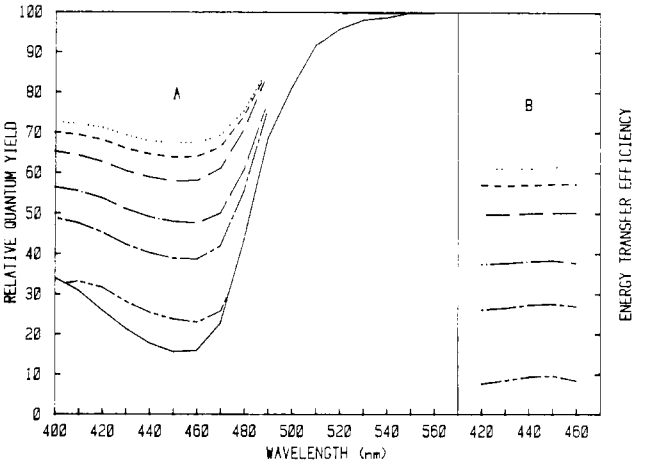

Figure 2. Corrected optically dense excitation spectra for Rh101 and $[Ru(bpy)_3]^{2+}$ in deoxygenated methanol (A). The solid line is the fractional absorbance of the Rh101. In all cases, [Rh101] = [$[Ru(bpy)_3]^{2+}$]. The Rh101 concentrations are 0.25 mM (——), 0.5 mM (——), 0.75 mM (—·—), 1.0 mM (——), 1.5 mM (– – –), and 2.0 mM (···). The ϕ_{ET}'s calculated as functions of wavelength (every 10 nm) are shown in B.

All decay curves yielded semilogarithmic plots which were linear over at least 2 mean lives.

The electrochemical data were obtained in acetonitrile for Rh101 or methanol (0.1 M tetrabutylammonium perchlorate or tetrafluoroborate) using a Bioanalytic Model CV-1A cyclic voltammetry system. The reference electrodes were Ag/(0.1 M $AgNO_3$ in acetonitrile) or a standard calomel electrode (SCE), and the working electrode was glassy carbon or platinum. All data are reported with respect to a SCE. Where required, the correction was obtained by measuring the voltage difference between the SCE and the $Ag/AgNO_3$ electrodes in the test solution. The typical differences of +0.335 to +0.345 V were added to the values measured relative to the $Ag/AgNO_3$ reference. Potentials are estimated to be accurate to ±20 mV. Results were independent of the reference electrode.

Results

Table I summarizes the electrochemical half-cell potentials relative to the SCE for the oxidation ($\mathcal{E}^0(S^+/S)$) and reduction ($\mathcal{E}^0(S/S^-)$) of $[Ru(bpy)_3]^{2+}$ and the dyes. The values were independent of the solvent for Rh101. The state energy, E_0, for the lowest excited singlet state of each dye is included. These values were derived by plotting the absorption spectrum of the lowest energy singlet transition and the corrected emission spectrum on the same plot; both curves were normalized to the same peak heights. A good mirror image existed in all cases, and E_0 was taken as the energy of the crossing of the two curves. For $[Ru(bpy)_3]^{2+}$ the state energy, E_0, of the sensitizing level was taken from the literature.[21]

Figure 2 shows a typical data set from the quantum counter comparator. Each corrected excitation spectrum is normalized to unity at long wavelengths where only the dye absorbs. The solid line is the fractional absorbance of the dye; the $[Ru(bpy)_3]^{2+}$ absorbs the remainder of the light. Since equimolar mixtures of $[Ru(bpy)_3]^{2+}$ and the dye were used, this same fractional absorbance applies to each dye-complex concentration. In all cases

(19) Van Houten, J.; Watts, R. J. *J. Am. Chem. Soc.* **1976**, *98*, 4853.
(20) Turley, T. J., M. S. Thesis, University of Virginia, Charlottesville, Va., 1979.
(21) Addington, J. W.; Demas, J. N. *J. Am. Chem. Soc.* **1976**, *98*, 5800.

most of the 450-cm exciting light was absorbed by the Ru(II) complex. In the absence of energy transfer from $*[Ru(bpy)_3]^{2+}$ to the dye, all the normalized excitation spectra would match the fractional absorbance of the dye. Alternatively, if there were ~100% energy transfer, all the curves would be unity at all wavelengths. The more closely the observed curves approach the latter case, the higher the energy transfer efficiency.

Figure 2 clearly shows the increase in energy transfer efficiency with increasing dye concentration. Because the donor luminescence can produce a measurable detector signal, however, corrections for this trivial effect must be made. We now develop the equation used to evaluate energy transfer efficiencies, ϕ_{ET}'s, and describe how the necessary ancillary parameters were obtained.

The observed sample signal strength, I, arises from dye and donor luminescence and depends on excitation wavelength. I is given by

$$I \propto TK_D F_D(1 - \phi_{ET}) + K_A F_A + K_A F_D \phi_{ET} \quad (1)$$

where F_D and F_A are the fraction of the excitation light absorbed by the donor and the acceptor, respectively. K_D and K_A are the relative responses of the detector to the pure donor and acceptor luminescences, respectively. These values correspond to intensities measured from optically dense donor or acceptor solutions using the same excitation conditions. T is the effective transmittance of the acceptor in the mixture to the donor's emission. A similar term for the acceptor's emission is unnecessary as the donor is transparent to the dye's emission. T, K_D, and K_A are assumed to be independent of excitation wavelength. The first term of eq 1 is the signal contributed by the donor emission; both donor–acceptor energy transfer and absorption of the donor's emission by the acceptor reduce this signal. The second term is the signal contribution from direct acceptor excitation. The third term arises from the sensitized acceptor emission.

In eq 1 the trivial process of absorption of the donor's emission by the acceptor followed by reemission is assumed to be negligible. This is a reasonable assumption. The error cannot exceed the donor's photon yield which is appreciably less than 10%. Further, eq 1 assumes that all donor quenching proceeds by energy transfer to the acceptor which is experimentally verified (vide infra). Also, eq 1 requires that the photon yield of the donor and acceptor be wavelength independent; this assumption is borne out for the systems examined here.

Evaluation of ϕ_{ET} in eq 1 requires elimination of the proportionality constant. Rather than trying to use an external standard, which would require very reproducible placement of cells, we chose to use the fluorescent dye in each mixture as an internal reference. This was done by taking the ratio, R, of the signal at short wavelengths, where both donor and acceptor absorb, to the signal at long wavelength where only the acceptor absorbs:

$$R = I_S/I_L \quad (2)$$

where I_S and I_L refer to the corrected signals from short and long wavelength excitation, respectively. ϕ_{ET} can then be evaluated from:

$$\phi_{ET} = \{RF_A - F_D TK - F_A\}/\{F_D - F_D TK\} \quad (3a)$$

$$K = K_D/K_A \quad (3b)$$

We turn now to the evaluation of K, F_A, F_D, and T.

K_D/K_A was obtained by replacing the sample cell with either a pure donor or pure acceptor sample and measuring the emission signals. The ratio of the donor to acceptor signals was K_D/K_A. The acceptor signals depended on the dye concentration because of self-absorption from overlap of the dye's emission with its absorption. Therefore, this measurement was done for each acceptor concentration.

F_A and F_D were calculated from the measured sample absorption spectra using

$$F_D = A_D/(A_D + A_A) \quad (4a)$$

$$F_A = 1 - F_D \quad (4b)$$

where A_D and A_A are the absorbances per centimeter of the donor and acceptor solutions, respectively. Equations 4 were valid because the solutions were optically dense.

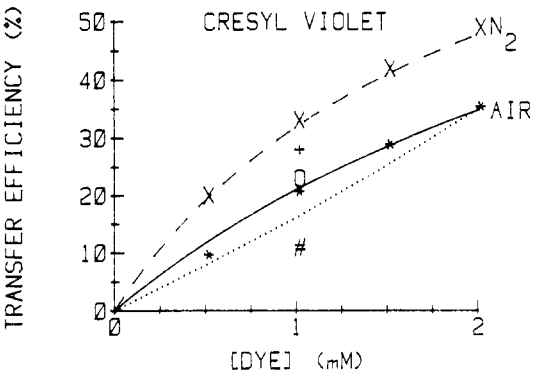

Figure 3. Energy-transfer efficiencies for the Cresyl Violet–$[Ru(bpy)_3]^{2+}$ system: (×) deoxygenated methanol, (*) aerated methanol, (+) deoxygenated ethylene glycol, (○) aerated ethylene glycol, (#) glycerol; (– – –) least-squares fit for deoxygenated methanol using eq 13, (—) least-squares fit for aerated methanol using $\phi_{ET}^0 = 1.00$, (···) calculated Förster energy-transfer curve for glycerol.

T was more difficult to evaluate. The detector, with a strongly wavelength dependent sensitivity curve, sees the donor's broadband emission filtered through the acceptor's broad absorption band. It was not possible to directly evaluate T from the phototube's spectral sensitivity curve coupled with the donor's emission and the acceptor's absorption spectra. Therefore, we measured T empirically using the arrangement of Figure 1B. The sample cell closest to the excitation source was filled with pure donor solution. Two detector readings were taken. In the first, pure water was placed in the filter cell while in the second a pure dye solution was used. The ratio of the second to first reading was T for the dye concentration used. T was determined for each dye concentration. In the energy-transfer experiments this treatment assumes that virtually all of the sample emission originated at the front surface of the excitation cell. This condition was satisfied except for the very lowest concentrations, although even here the solutions were optically dense and errors should be small.

Figure 2 also shows the quantitative ϕ_{ET}'s calculated at different excitation wavelengths for the Rh101 system. ϕ_{ET} is independent of excitation wavelength within experimental error. Similar experimental plots were obtained for the other dyes. Solvent viscosity as well as oxygen and dye concentrations affect ϕ_{ET}'s as shown in Figures 3, 4, and 5 for CV, NBA, and OX1. Similar plots for Rh101 are displayed elsewhere.[15]

The following values were obtained for luminescence photon yields of $[Ru(bpy)_3]^{2+}$ in deoxygenated, aerated, and oxygen-saturated solutions, respectively: ϕ = 0.0582, 0.015, 0.0048 (methanol); ϕ = 0.0766, 0.066, 0.039 (ethylene glycol). For glycerol, ϕ = 0.0836 independent of the degree of oxygenation. The lifetimes of $[Ru(bpy)_3]^{2+}$ in deoxygenated and air-saturated solvents were 765 and 217 ns (methanol), 844 and 681 ns (ethylene glycol), and 888 and 888 ns (glycerol).

The Förster critical transfer distances, R_0's, for dipole–dipole resonance transfer were calculated from[22,23]

$$R_0 = \left[\frac{900 \ln 10 K^2 \phi}{128 \pi^5 n^4 N} \int I_\lambda \epsilon_\lambda \lambda^4 \, d\lambda \right]^{1/6} \quad (5)$$

K^2 accounts for the angle between the transition moment vectors of the donor and the acceptor molecule and was assumed equal to 2/3 which is appropriate for positionally fixed, randomly oriented, but freely rotating molecules. ϕ is the donor's photon yield in the absence of energy transfer, n is the solvent's refractive index, and N is Avogadro's number. The integral is the overlap integral

(22) Latt, S. A.; Cheung, H. T.; Blout, E. R. *J. Am. Chem. Soc.* **1965**, *87*, 995.

(23) Birks, J. B. "Photophysics of Aromatic Molecules"; Wiley-Interscience: New York, 1970.

Table II. Energy-Transfer Properties of Dye-$[Ru(bpy)_3]^{2+}$ Systems

	deoxygenated				air-saturated		
dye	ϕ_{ET}^0 (%)	R_0 (Å)	K_{sv} (M^{-1})	$k_2 \times 10^{-9}$ (M^{-1} s^{-1})	R_0 (Å)	K_{sv} (M^{-1})	$k_2 \times 10^{-9}$ (M^{-1} s^{-1})
Rhodamine 101							
methanol	98 ± 6	27	650	0.85	22	220	1.0
ethylene glycol			470	0.55		280	0.41
glycerol						65	0.07
Cresyl Violet							
methanol	105 ± 9	37	510	0.67	30	265	1.2
ethylene glycol		40	390	0.46	39	280	0.41
glycerol					40	110	0.12
Nile Blue A							
methanol	102 ± 2	41	1890	2.5	33	720	3.3
ethylene glycol		40	1040	1.2	40	570	0.84
glycerol					42	250	0.28
Oxazine 1							
methanol	106 ± 3	44	1920	2.5	35	810	3.7
ethylene glycol		44	880	1.0	43	670	1.0
glycerol					44	280	0.31

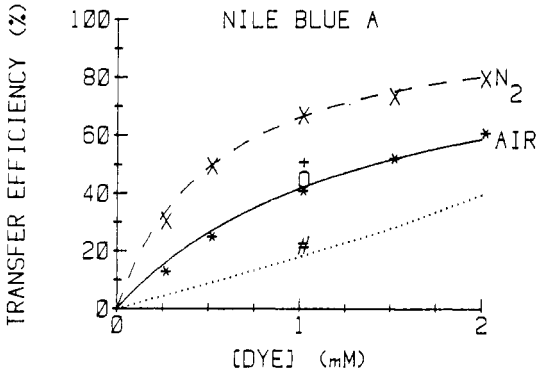

Figure 4. Energy-transfer efficiencies for the Nile Blue A-$[Ru(bpy)_3]^{2+}$ system: (×) deoxygenated methanol, (*) aerated methanol, (+) deoxygenated ethylene glycol, (O) aerated ethylene glycol, (#) glycerol; (– – –) least-squares fit for deoxygenated methanol using eq 13, (—) least-squares fit for aerated methanol using $\phi_{ET}^0 = 1.00$, (···) calculated Förster energy-transfer curve for glycerol.

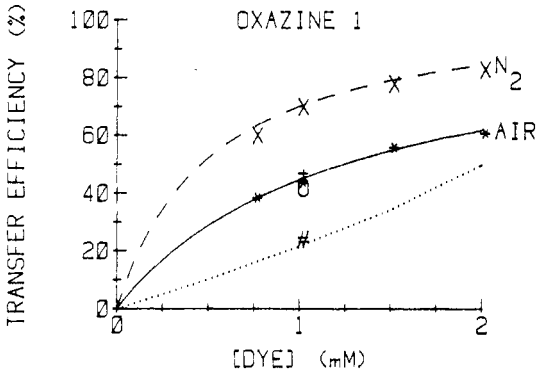

Figure 5. Energy-transfer efficiencies for the Oxazine 1-$[Ru(bpy)_3]^{2+}$ system: (×) deoxygenated methanol, (*) aerated methanol, (+) deoxygenated ethylene glycol, (O) aerated ethylene glycol, (#) glycerol; (– – –) least-squares fit for deoxygenated methanol using eq 13, (—) least-squares fit for aerated methanol using $\phi_{ET}^0 = 1.00$, (···) calculated Förster energy-transfer curve for glycerol.

between the donor's corrected luminescence spectrum, I_λ, and the acceptor's absorption spectrum. I_λ is normalized to unity, and ϵ_λ is the acceptor's molar extinction coefficient. Integration is over the entire emission band. R_0's calculated for the $[Ru(bpy)_3]^{2+}$–dye systems are given in Table II.

Discussion

Energy-transfer efficiencies are sensitive to dye and oxygen concentrations as well as solvent viscosity. We now use this information to interpret our results.

In highly viscous glycerol, at the same dye concentrations, ϕ_{ET}'s are greatly reduced compared to the results in deoxygenated methanol. Further, the ϕ_{ET}'s for glycerol solvents correspond well to the theoretical values obtained by the Förster resonance mechanism.[23] See Figures 3–5. In the less viscous methanol and ethylene glycol, however, the Förster equation seriously underestimates ϕ_{ET}. Therefore, both dipole–dipole interactions and diffusion probably play important roles in the energy-transfer processes.

The importance of diffusion is demonstrated when one considers the mean diffusion distance of $*[Ru(bpy)_3]^{2+}$ compared with the R_0's. The mean diffusion distance is given by $(2D\tau)^{1/2}$ where D is the diffusion coefficient and τ is the excited-state lifetime. In methanol $(2D\tau)^{1/2}$ varies from 120 to 240 Å on going from air-saturated to deoxygenated conditions.[4,24] In ethylene glycol, the corresponding values are 41 to 45 Å, and in glycerol the value is 6.5 Å independent of oxygenation. In glycerol $(2D\tau)^{1/2} \ll R_0$ which indicates that the donors are essentially positionally fixed during their excited-state lifetime. Thus, for glycerol the necessary conditions for accurate application of the Förster equation with fixed donor and acceptor apply, and the agreement between the calculated and observed energy-transfer efficiencies for glycerol is as expected. In methanol and ethylene glycol, however, $(2D\tau)^{1/2}$ is comparable to or much greater than R_0 which indicates that diffusion must play an important role in the energy-transfer processes.

In the more fluid solutions there are several possible mechanisms for energy transfer. These include: (1) donor emission followed by reabsorption by the acceptor; (2) collisional exchange energy transfer from the donor's CT state to the dye triplet state followed by triplet–triplet (T–T) annihilation to form a singlet excited dye molecule; (3) excited-state electron transfer followed by chemical generation of the excited dye; (4) diffusion-assisted dipole–dipole Förster resonance energy transfer; (5) collisional exchange energy transfer directly from the donor's CT state to the dye singlet manifold.

We promptly rule out the trivial emission–reabsorption pathway. The maximum efficiency is the donor's photon yield which is <10%. Thus, the observed high ϕ_{ET}'s cannot be accounted for by the trivial pathway.

T–T annihilation can be ruled out. The maximum energy transfer efficiency for this mechanism is 0.5 which falls well below the observed yields for OX1 and NBA in deaerated solutions. Further, the limiting yields extrapolated to infinite dye concentrations (vide infra) for all the dyes are unity which is, again, inconsistent with T–T annihilation. Finally, in air-saturated solutions at the low excitation conditions used, O_2 quenching of the dye triplet states would suppress virtually all T–T annihilation

(24) The diffusion coefficient was assumed to be inversely proportional to the solvent macroscopic viscosity. D for water was taken from the literature.

and, thus, energy transfer. While O_2 reduces the observed yields, the effect is small and, as we shall show, can be modeled successfully without invoking T–T annihilation.

Chemical generation of $^1O_2$ has been proposed by Lin and Sutin in quenching of the excited states of metal complexes.[4] Their proposed mechanism, which is applicable to the current work, is

$$*D + A \rightarrow *D|A \rightarrow D^{\pm}|A^{\mp} \quad (6a)$$

$$D^{\pm}|A^{\mp} \rightarrow D|*A \quad (6b)$$

$$D|*A \rightarrow D + *A \quad (6c)$$

where the | denotes an encounter pair and $D^{\pm}$ and $Q^{\mp}$ represent the oxidized or reduced forms of the donor and acceptor, respectively. For this mechanism to be operative two conditions must be satisfied. First, the excited sensitizer must be a powerful enough oxidant or reductant so that one of the reactions

$$*D + A \rightarrow D^+ + A^- \quad \Delta\mathcal{E}_{7a} \quad (7a)$$

$$*D + A \rightarrow D^- + A^+ \quad \Delta\mathcal{E}_{7b} \quad (7b)$$

can proceed efficiently. To be efficient the rate constant must be large; this requires that $\Delta\mathcal{E}$ for the reaction must be positive by at least 0.1 V. Second, for a reaction which is efficient, the energy released by the back electron-transfer reaction

$$D^+ + A^- \rightarrow D + A \quad \Delta\mathcal{E}_{8a} \quad (8a)$$

$$D^- + A^+ \rightarrow D + A \quad \Delta\mathcal{E}_{8b} \quad (8b)$$

must equal or exceed the singlet excited-state energy of A.

The energies of the oxidative and reductive quenching process of reactions 7 are given by

$$\Delta\mathcal{E}_{7a} = -*\mathcal{E}^0(D^+/*D) + \mathcal{E}^0(A/A^-) \quad (9a)$$

$$\Delta\mathcal{E}_{7b} = +*\mathcal{E}^0(*D/D^-) - \mathcal{E}^0(A^+/A) \quad (9b)$$

where $\mathcal{E}^0(D^+/*D)$ and $\mathcal{E}^0(*D/D^-)$ are the standard half-cell potentials for oxidation and reduction of the excited state, respectively. These quantities are evaluated from

$$*\mathcal{E}^0(D^+/*D) = \mathcal{E}^0(D^+/D) - {}^DE_0 \quad (10a)$$

$$*\mathcal{E}^0(*D/D^-) = \mathcal{E}^0(D/D^-) + {}^DE_0 \quad (10b)$$

where ${}^DE_0$ is the state energy of the donor's sensitizing CT level. From the data of Table I we find $*\mathcal{E}^0(D^+/*D) = -0.85$ V and $*\mathcal{E}^0(*D/D^-) = 0.78$ V.

Similarly $\Delta\mathcal{E}_{8a}$ and $\Delta\mathcal{E}_{8b}$ are given by

$$\Delta\mathcal{E}_{8a} = +\mathcal{E}^0(D^+/D) - \mathcal{E}^0(A/A^-) \quad (11a)$$

$$\Delta\mathcal{E}_{8b} = -\mathcal{E}^0(D/D^-) + \mathcal{E}^0(A^+/A) \quad (11b)$$

Table I summarizes the derived $\Delta\mathcal{E}$'s. These results demonstrate that an electron-transfer pathway for energy transfer is not a possible explanation of the observed energy transfer.

We consider first CV, NBA, and OX1. From Table I we see that $*[Ru(bpy)_3]^{2+}$ is far too weak (by 0.3 V) an excited-state oxidant to oxidize these dyes. Pathway 7b and, thus, 8b can be ruled out for generation of the excited dye. $*[Ru(bpy)_3]^{2+}$ is quite capable of reducing the dyes. However, the back-electron-transfer reaction of eq 8a falls 0.2 V short of supplying the necessary energy to excite the singlet state of the dyes. Therefore, the observed efficient sensitized luminescences of CV, NBA, and OX1 cannot arise by the electron-transfer pathways of eq 6.

For Rh101, pathway 7a is energetically unfavorable by 0.3 V and thus not available. E_0 is slightly above the sensitizing level of $[Ru(bpy)_3]^{2+}$, and the energy produced by reaction 8b is 0.1 V too small to excite the singlet state of the dye. We conclude that for Rh101 an electron-transfer mechanism for energy transfer is not possible.

We now justify our assumption of a possible exchange-energy-transfer mechanism. The CT excited states of Ru(II) complexes with α-diimine ligands have been widely described as triplet states. If this statement is correct, an exchange singlet-energy transfer from the CT state of $[Ru(bpy)_3]^{2+}$ to the dyes would be spin forbidden and could be ruled out. Crosby and co-workers,[6,7] however, have demonstrated that the CT states must, in fact, be described as spin–orbit states with considerable amounts of both singlet and triplet character. Thus, both singlet and triplet exchange interactions are possible.

We are, therefore, left with Förster and direct singlet energy transfer by a collisional exchange interaction. In either case, at least in low viscosity methanol, the data can be approximated as a diffusional process and described by

$$D \xrightarrow{h\nu} *D \quad \phi' \quad (12a)$$

$$*D \xrightarrow{k_1} D + h\nu \text{ or } D + A \quad (12b)$$

$$*D + A \xrightarrow{k_{et}} D + *A \quad \phi_{ET} \quad (12c)$$

$$*D + A \xrightarrow{k_q} D + A + \Delta \text{ or reaction} \quad (1 - \phi_{ET}) \quad (12d)$$

where A is the acceptor dye, ϕ' is the efficiency of population of the sensitizing level of D following excitation, and ϕ_{ET} is the singlet energy-transfer efficiency. This model yields:

$$1/\phi_{ET} = (1/\phi_{ET}{}^0K_{sv})(1/[A]) + (1/\phi'\phi_{ET}{}^0) \quad (13a)$$

$$K_{SV} = k_2\tau_0 \quad (13b)$$

$$k_2 = k_{et} + k_q \quad (13c)$$

$$\tau_0 = 1/k_1 \quad (13d)$$

$$\phi_{ET}{}^0 = \phi'[k_{et}/(k_q + k_{et})] \quad (13e)$$

where $\phi_{ET}{}^0$ is the limiting energy-transfer efficiency at $[A] = \infty$. K_{SV} and k_2 are the Stern–Volmer and bimolecular quenching constants, respectively. τ_0 is the unquenched donor lifetime.

Plots of $1/\phi_{ET}$ vs. $1/[A]$ were linear as required by eq 13. Table II summarizes the resultant $\phi_{ET}{}^0$'s and K_{SV}'s derived for the deaerated solutions from eq 13. Estimated errors in $\phi_{ET}{}^0$'s are standard deviations derived assuming a standard deviation in the measured ϕ_{ET}'s of 0.02. The $\phi_{ET}{}^0$'s are all within experimental error of unity.

In the aerated solutions, the $\phi_{ET}{}^0$'s, estimated from eq 13, were reasonably close to unity although they all appeared to be somewhat above unity. The ϕ_{ET}'s were, however, lower which reduced the accuracy of the $\phi_{ET}{}^0$'s. We do not report $\phi_{ET}{}^0$'s for the aerated solutions. To make more accurate estimates of the K_{SV}'s in the aerated solutions, we assumed that the $\phi_{ET}{}^0$'s were 1.00 and adjusted the K_{SV}'s in eq 13 to minimize the sums of the squares of the residuals between the observed and calculated ϕ_{ET}'s.

For glycerol and ethylene glycol solutions we made measurements only at dye and donor concentrations of 10^{-3} M. K_{SV} was calculated from eq 13 assuming $\phi_{ET}{}^0 = 1.00$.

The fits to the experimental data using the $\phi_{ET}{}^0$'s and K_{SV}'s are shown in Figure 3–5 for the deoxygenated solutions along with the best fits for the air-saturated solutions (${}^0\phi_{ET} = 1.00$). The root-mean-square deviations of 0.01–0.015 support our estimated uncertainties in the ϕ_{ET}'s used in the error calculations for $\phi_{ET}{}^0$. Clearly, a simple bimolecular diffusion model fits the methanol data within experimental error.

Bimolecular rate constants, k_2 (eq 13b), are summarized in Table II. Except for Rh101, the rate constants differ noticeably between the aerated and deoxygenated solutions; these variations appear well beyond our experimental error.

Before discussing the mechanism of energy transfer, we make an important observation about the formation efficiency for populating the sensitizing CT state of $[Ru(bpy)_3]^{2+}$. An early claim was made that ϕ' was less than unity and electron- and energy-transfer studies seemed to support this. A growing body of experimental data from different chemical and spectroscopic sources indicate, however, that $\phi' = 1.00$ (see ref 25 for a discussion of these observations). Our current results were derived

(25) Demas, J. N.; Taylor, D. G. *Inorg. Chem.* **1979**, *18*, 3177.

Table III. Comparison of Calculated and Observed Energy-Transfer Rate Constants

	deoxygenated		air-saturated	
acceptor	$k_2 \times 10^{-9}$ (M^{-1} s^{-1})	k_2(För) $\times 10^{-9}$ [a] (M^{-1} s^{-1})	$k_2 \times 10^{-9}$ (M^{-1} s^{-1})	k_2(För) $\times 10^{-9}$ [b] (M^{-1} s^{-1})
Rhodamine 101	0.85	0.1	1.0	0.2
Cresyl Violet	0.67	0.67	1.2	1.2
Nile Blue A	2.5	1.2	3.3	2.2
Oxazine 1	2.5	2.0	3.7	3.6

[a] D_{12} = 14.7 Å. [b] D_{12} = 11.7 Å.

from an entirely different type of measurement and further support the unity value of ϕ' for $[Ru(bpy)_3]^{2+}$ and, by analogy, other α-diimine complexes of platinum metals.[26]

A diffusional picture is reasonable for the methanol data. The mean diffusion distances of the unquenched excited state of $[Ru(bpy)_3]^{2+}$ are ~120 to 240 Å for air and deoxygenated methanol respectively. This is typically 3–6 times R_0. Thus, diffusional motion must play an important part in the excited-state interaction. The observation of a diffusional component to the quenching does not, however, prove exchange energy transfer. Even in the absence of contact transfer, diffusional motion will continually bring new excited molecules within R_0 where Förster transfer can occur. The real question is to what extent does contact exchange transfer compete with Förster transfer.

Rigorous closed-form solutions to the general diffusion problem with both Förster and exchange energy transfer are not available, although complex numerical solutions are, in principle, possible.[29] In the absence of temporal decay information, we adopt the approximate solution of Kurskii and Selivanenko[30] which is suitable for low viscosity solutions. Their low viscosity limit applies rigorously to less viscous media than used here with mean diffusion distances of $>30R_0$; however, methanol has a low enough viscosity that the Kurskii–Selivanenko (KS) solution should be approximately correct.

The decay function predicted by the KS theory includes a normal pseudo-first-order term plus a transient $t^{1/2}$ term. In view of the excellent fit of our experimental ϕ_{ET} data to a simple diffusional model, we infer that the transient $t^{1/2}$ terms can be neglected. Under these conditions the observed bimolecular energy transfer expression is

$$k_2 = k_2(\text{exc}) + k_2(\text{För}) \quad (14a)$$

$$k_2(\text{För}) = 6.023 \times 10^{20}(4\pi/12\tau_0)(R_0^2/D_{12})^3 \quad (14b)$$

where k_2(exc) is the normal contact exchange transfer rate constant given by the Smoluchowski equation and k_2(För) is the diffusion-assisted Förster transfer rate constant. D_{12} is the center-to-center molecular separation or contact distance, R_0 is the Förster critical distance, and τ_0 is the unquenched donor lifetime. As given k_2(För) has units of M^{-1} s^{-1} if R_0 and D_{12} are in centimeters and τ_0 is in seconds.

In this model k_2 cannot be less than k_2(För). If k_2 exceeds k_2(För), then the excess rate arises from contact exchange transfer. We now demonstrate how to estimate k_2(För) for the current systems.

We need D_{12} to evaluate k_2(För). Our dyes are large planar molecules with similar structures. We, therefore, assume that they have similar D_{12}'s. Since $k_2 > k_2$(För), we can obtain a lower limit for D_{12} by taking the dye with the lowest k_2 and assuming $k_2 = k_2$(För). Using the deoxygenated CV system, we find D_{12} = 14.7 Å. Table III compares the k_2(För)'s and the observed k_2's.

The KS theory will be less accurate for the air-saturated values since the mean diffusion distances more closely approach R_0. Repeating the calculation for the aerated CV solution, we calculate D_{12} = 11.7 Å. The observed k_2's and the calculated k_2(För) for the aerated solutions are also included in Table III.

For both aerated and deaerated solutions, the observed k_2's match reasonably well the k_2(För) for NBA and OX1, although the k_2(För)'s for the deoxygenated case are too low by ~0.6–1.3 $\times 10^9$ m^{-1} s^{-1}. There is no question, however, that k_2(För) for Rh101 is many times lower than the observed k_2.

The good agreement between the k_2's calculated by the KS theory and the observed k_2's indicates that the dominant energy-transfer mechanism in the CV, OX1, and NBA systems is diffusion-assisted Förster transfer. For NBA and OX1, the similar discrepancies between k_2 and k_2(För), however, suggest that there is a component of contact exchange energy transfer. Given the approximations of the theory, a definitive statement about the presence of any contact singlet transfer is not possible for OX1 and NBA.

For Rh101, however, the discrepancy between k_2 and k_2(För) is so large that the dominant energy-transfer mechanism must be an exchange transfer. If we attempt to fit the Rh101 data with the KS theory we can only match the observed k_2 by assuming that D_{12} = 6.7 Å; this is an unrealistic interaction distance for Rh101 which is larger than CV, NBA, or OX1. Further, if we assume a universal D_{12} of 6.7 Å, we obtain k_2(För) = 7–21 $\times 10^9$ M^{-1} s^{-1} for the other dyes which greatly exceeds the observed values. We conclude that for Rh101 k_2(exc) ~ 1×10^9 M^{-1} s^{-1}. The discrepancies between k_2 and k_2(För) for NBA and OX1 suggest that k_2(exc) is also comparable for these dyes.

We comment briefly on the discrepancies between the D_{12}'s calculated for the deoxygenated and air-saturated methanol solutions. The KS theory only applies rigorously when $(2D\tau)^{1/2} > 30R_0$. For the deoxygenated solutions the mean diffusion range is ~6–8 times R_0's. For aerated methanol, however, the diffusion range is ~4–6 times R_0. Thus, we expect the theory to be less satisfactory for the aerated solution, and small variations in D_{12} calculated for the two media are not surprising.

The D_{12} values calculated by the KS theory are reasonable. The complex and dyes are large molecules. Further, $[Ru(bpy)_3]^{2+}$ probably exists largely as a divalent cation and the dyes as monovalent cations in methanol. Thus, for the KS model, the effective D_{12} is probably larger than the true physical contact distance because of electrostatic repulsions. Finally, k_2(exc) is at or below the diffusion-controlled limit. At the maximum ionic strength used, the Debye–Brønsted theory predicts diffusion-limited rate constants of 0.6–3.9 $\times 10^9$ M^{-1} s^{-1} for D_{12} = 12–20 Å. For D_{12} = 14 Å, k_2 (diffusion controlled) = 1.2×10^9 M^{-1} s^{-1} which is in excellent agreement with the observed value for Rh101.

The presence of such a large k_2(exc) for Rh101 and possibly for the other dyes indicates that exchange transfer is highly allowed. Thus, the sensitizing CT state of $[Ru(bpy)_3]^{2+}$ must possess a great deal of singlet character. We consider our current results as strongly supporting the Crosby et al.[6,7] spin–orbit model for CT states of platinum metal complexes. Our results also demonstrate that the wide use of the "triplet" label for these CT states should be abandoned and these states should be properly referred to as spin–orbit states. Finally, the term CT phosphorescence should be dropped and the emission properly referred to only as a luminescence.

We briefly address the question of why facile contact singlet energy transfer only occurs here for Rh101 even though it appears to be reasonably facile in the gas phase.[31] The answer is in the long times required for the reactants in a viscous solution to close to a contact distance. If R_0 is large, Förster transfer will occur before the distance can be covered. For ruthenium and osmium complexes with emitting CT states, the emissions are generally rather allowed which gives large R's for dyes capable of accepting

(26) A recent claim of subunity ϕ's for $[Ru(phen)_3]^{2+}$ has been made.[27] The experimental basis of this claim, however, rests on experiments which are in disagreement with results from our laboratory.[25,28]

(27) Sriram, R.; Hoffman, M. Z. *Chem. Phys. Lett.* **1982**, *85*, 572.

(28) Hauenstein, B. A.; Buell, S., unpublished results.

(29) (a) Elkana, Y.; Feitelson, J.; Kalchalski, E. *J. Chem. Phys.* **1968**, *48*, 2399. (b) Steinberg, I.; Katchalski, E. *Ibid.* **1968**, *48*, 2404. (c) Guarino, A. *J. Photochem.* **1979**, *11*, 273.

(30) Kurskii, Yu. A.; Selivanenko, A. S. *Opt. Spectrosc. (USSR)* **1960**, *8*, 340.

(31) Loper, G. L.; Lee, E. K. C. *J. Chem. Phys.* **1975**, *63*, 264.

energy. Thus, for solution measurements employing donors having reasonably allowed emissions, contact singlet exchange energy transfer will probably be uncommon.

Acknowledgment. We gratefully acknowledge the Air Force Office of Scientific Research (Chemistry) (Grant AFOSR 78-3590) and the donors of the Petroleum Research Fund, administered by the American Chemical Society. All lifetime measurements were performed on the University of Virginia laser facility which was purchased in part with NSF Grant CHE 77-09296.

Registry No. $[Ru(bpy)_3]^{2+}$, 15158-62-0; Rhodamine 101, 64339-18-0; cresyl violet, 18472-89-4; nile blue, 2381-85-3; oxazine 1, 24796-94-9.

Effects of Cyclic 8-π-Electron Conjugation in Reductively Silylated N-Heterocycles[1]

Wolfgang Kaim

Contribution from the Chemistry Department, J. W. Goethe-Universität, Niederurseler Hang, D-6000 Frankfurt am Main, West Germany. *Received December 28, 1981*

Abstract: A number of partly reduced N-heterocycles, **2–15**, have been prepared by reductive silylation of aromatic precursors. The *N*-silyl substituents stabilize unusual electronic structures such as the 1,4-dihydropyrazine system toward rearrangements. In addition, R_3Si substitution is likely to cause planarization at the amino nitrogen atoms. This may lead to cyclic 8-π-electron conjugation, as has been established, e.g., for 1,4-bis(trimethylsilyl)-1,4-dihydropyrazine (**2**). The experimental results obtained for **2** by comparative ^1H NMR and photoelectron spectroscopic studies are a distinct paratropism, an exceptionally low ionization potential, and an enormous difference between the first and second ionization energy. These effects confirm the predictions made for planar 1,4-dihydropyrazine on the basis of HMO calculations. Corresponding to the very low ionization potentials of most of the reduced compounds, persistent radical cations such as $\mathbf{2}^{+\cdot}$ have been readily obtained and were fully characterized by ESR spectroscopy. Modification of the 1,4-dihydropyrazine **2** by methyl substitution or by extension of the π system results in an attenuation of the 8-π- electron conjugation through steric and/or electronic factors. The flexibility of this system toward steric requirements can be related to the redox behavior of flavoenzymes.

For a variety of reasons, the 1,4-dihydropyrazine structural unit

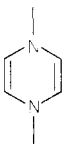

I

has attracted a great deal of attention: (1) It can be regarded as a potential "antiaromatic"[2] system due to the availability of 8 π electrons in a sterically constrained six-membered ring.[3-6] Such a system cannot deviate as much from planarity as the iso-π-electronic seven-[7,8] and eight-membered[9a] rings II and III.

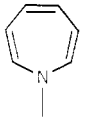

II

III

(2) The electronic structure of the cyclic six-center π-electron arrangement I may be conveniently described in terms of the familiar benzene HMO formalism.[9b,10] Calculations for planar 1,4-dihydropyrazine (**1**) have predicted the occupancy of an antibonding molecular orbital[9b] that would render such a compound extremely electron rich. (3) The 1,4-dihydropyrazine system is an essential constituent of biochemically important molecules, viz., of the 1,5-dihydroflavins IV[11-13] and of certain luciferins V.[14] (4)

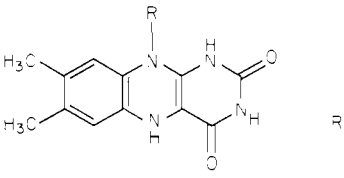

IV

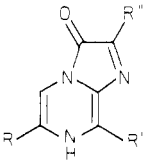

V

(1) Preliminary communications: Kaim, W. *Angew. Chem.* **1981**, *93*, 620, 621; *Angew. Chem., Int. Ed. Engl.* **1981**, *20*, 599, 600.

(2) Breslow, R. *Angew. Chem.* **1968**, *80*, 573; Angew. *Chem., Int. Ed. Engl.* **1968**, *7*, 565; *Acc. Chem. Res.* **1973**, *6*, 393. Dewar, M. J. S. *Angew. Chem.* **1971**, *83*, 859; *Angew. Chem., Int. Ed. Engl.* **1971**, *10*, 761.

(3) Chen, S. J.; Fowler, F. W. *J. Org. Chem.* **1971**, *36*, 4025.

(4) (a) Lown, J. W.; Akhtar, M. H. *J. Chem. Soc., Chem. Commun.* **1972**, 829. (b) *Ibid.* **1973**, 511. (c) *J. Chem. Soc., Perkin Trans. 1* **1973**, 683. (d) Lown, J. W.; Akhtar, M. H.; McDaniel, R. S. *J. Org. Chem.* **1974**, *39*, 1998.

(5) (a) Schmidt, R. R. *Angew. Chem.* **1975**, *87*, 603; *Angew. Chem., Int. Ed. Engl.* **1975**, *14*, 581. (b) Schmidt, R. R.; Dimler, M.; Hemmerich, P. *Chem. Ber.* **1976**, *109*, 2395.

(6) Cf. the failure to generate the "antiaromatic" benzene dianion: Stevenson, G. R.; Zigler, S. S.; Reiter, R. C. *J. Am. Chem. Soc.* **1981**, *103*, 6057.

(7) Hafner, K. *Angew. Chem., Int. Ed. Engl.* **1964**, *3*, 165. Vogel, E.; Günther, H. *Ibid.* **1967**, *6*, 385. Maier, G. *Ibid.* **1967**, *6*, 402. Paquette, L. A. *Ibid.* **1971**, *10*, 11. For structure determinations of 1*H*-azepine derivatives see: Lindner, H. J.; von Gross, B. *Chem. Ber.* **1972**, *105*, 434 and literature cited therein.

(8) Vogel, E.; Altenbach, H. J.; Drossard, J. M.; Schmickler, H.; Stegelmeier, H. *Angew. Chem.* **1980**, *92*, 1053; *Angew. Chem., Int. Ed. Engl.* **1980**, *19*.

(9) Streitwieser, A., Jr. "Molecular Orbital Theory for Organic Chemists"; Wiley: New York, 1961: (a) pp 282–284 and literature cited therein; (b) pp 275–277.

(10) Heilbronner, E.; Bock, H. "The HMO-Model and its Application"; Wiley: London; Verlag Chemie: Weinheim/Bergstr., 1976: (a) Vol. I, pp 191 and 233; (b) Vol. III; (c) Vol. I, p 198.

(11) Hemmerich, P.; Veeger, C.; Wood, H. C. S. *Angew. Chem.* **1965**, *77*, 699; *Angew. Chem., Int. Ed. Engl.* **1965**, *4*, 671. Hemmerich, P. In "Bioinorganic Chemistry 2"; Raymond, K. N., Ed.; American Chemical Society: Washington, DC, 1977; n 162, p 312. Walsh, C. *Acc. Chem. Res.* **1980**, *13*, 148.

(12) (a) ^1H NMR studies: Tauscher, L.; Ghisla, S.; Hemmerich, P. *Helv. Chim. Acta* **1973**, *56*, 630. (b) ^{13}C NMR studies: van Schagen, C. G.; Müller, F. *Ibid.* **1980**, *63*, 2187. (c) X-ray crystallographic studies: Norrestam, R.; von Glehn, M. *Acta Crystallogr., Sect. B* **1972**, *B 28*, 434. (d) ESR/ENDOR studies of radical cations: Bock, M.; Lubitz, W.; Kurreck, H.; Fenner, H.; Grauert, R. *J. Am. Chem. Soc.* **1981**, *103*, 5567. (e) Electrochemical studies: Draper, R. D.; Ingraham, L. L. *Arch. Biochem. Biophys.* **1968**, *125*, 802. Meisel, D.; Neta, P. *J. Phys. Chem.* **1975**, *79*, 2459. (f) PE spectra and ab initio calculations: Palmer, M. H.; Simpson, I.; Platenkamp, R. J. *J. Mol. Struct.* **1980**, *66*, 243.

(13) Bruice, T. C.; Yano, Y. *J. Am. Chem. Soc.* **1975**, *97*, 5263. Williams, R. F.; Shinkai, S. S.; Bruice, T. C. *Ibid.* **1977**, *99*, 921. Chan, T. W.; Bruice, T. C. *ibid.* **1977**, *99*, 7287.

0002-7863/83/1505-0707$01.50/0